Journal of Power Sources 196 (2011) 6242–6248

Contents lists available at ScienceDirect

Journal of Power Sources

journal homepage: www.elsevier.com/locate/jpowsour

Critical importance of humidification of the anode in miniature air-breathing polymer electrolyte membrane fuel cells

Simon Hamel*, Luc G. Fréchette

Université de Sherbrooke, Dept of Mechanical Engineering, 2500 Boul. Université, Sherbrooke, Québec J1K 2R1, Canada

ARTICLE INFO

Article history:
Received 24 January 2011
Received in revised form 6 April 2011
Accepted 7 April 2011
Available online 13 April 2011

Keywords:
PEMFC
Natural convection
Anode drying
Water management
Flooding

ABSTRACT

Although water management at the cathode is known to be critical in miniature polymer electrolyte membrane fuel cells (mPEMFCs), this study shows that control of water transport towards the anode is a determining factor to increase air-breathing mPEMFC performances. An analytical 1D model is developed to capture the water transport and water content profile in the membrane. It shows that drying at the anode and flooding at the cathode can happen simultaneously, mainly due to dominant electro-osmotic drag at low cell temperatures. Experimental results demonstrate that injecting water at the anode, at a rate of 3 times the amount produced at the cathode, increases the cell performances at high current densities. By this method, the limiting current and maximum power densities have been raised by 100% and 30% respectively.

1. Introduction

Polymer electrolyte membrane fuel cells (PEMFCs) are well suited for small portable applications, given their solid electrolyte, quick start-up and low operating temperature [1]. Devices like laptops, cell phones or wireless sensors need compact and lightweight power sources able to produce from a few watts to milliwatts within a fraction of the device's volume.

Because of the low output power and small scale of miniature cells (mPEMFCs), external components such as pumps or fans become less attractive. They would significantly reduce the system efficiency and make it less portable in size. Therefore, it is more practical to rely on natural convection at the cathode of mPEMFCs (i.e. using an air-breathing cathode) and use a dead-ended fuel supply at the anode. However, water management becomes particularly challenging without forced gas flows. Evaporation of the water generated at the cathode may not be sufficient, leading to an accumulation of liquid water near the electrodes that block gas pathways. This challenge is even greater for mPEMFCs since they typically operate at relatively low temperatures (near ambient) due to the small ratio of the active area (<5 cm^2) of mPEMFCs compared to the volume of their packaging.

These restrictions often cause poor water management and low cell performances. The maximum operating current can be limited by mass transfer, such as a deficient oxygen supply due to cathode flooding, or by excessive resistances, such as ionic resistance caused by membrane or anode drying. Since liquid water is generally visible at the cathode surface when the potential of the air-breathing mPEMFC falls, flooding is often pointed out as the principal factor in voltage loss. To address this problem, many approaches have been developed over the years. For example, standard or microfabricated [2,3] gas diffusion layers (GDL) can be applied on the cathode to wick the water out of the electrode and open pathways for oxygen diffusion. Fabian et al. [4] have used an electro-osmotic pump to clear the cathode of water for a low temperature air-breathing mPEMFC with interesting results. Still, few studies have taken into consideration the role of the anode in water management because it is considered that drying of the anode will not occur simultaneously with flooding at the cathode. Nevertheless, Jung et al. [5] has shown that it is possible to improve air-breathing mPEMFC performances by adding a hydrophilic component in the anode. It was concluded that the improvements were due to increased humidification of the anode and not to the water removal from the cathode. Furthermore, Chu and Jiang [6] has also shown that feeding humidified H_2 to the anode slightly improved PEMFC performances, even at low temperatures. This suggests that anode drying happens even at ambient conditions when the cathode is flooding.

In this study, a simple steady-state analytical model of water transport through a mPEMFC is used to capture potential drying at the anode and flooding at the cathode. Results are then validated experimentally by observing the impact of anode humidification on the performance of a 2 cm^2 air-breathing cell.

* Corresponding author. Tel.: +1 819 821 8000x63179; fax: +1 819 821 7163.
E-mail address: Simon.hamel@Usherbrooke.ca (S. Hamel).

0378-7753/$ – see front matter © 2011 Elsevier B.V. All rights reserved.
doi:10.1016/j.jpowsour.2011.04.020

Nomenclature

A	active area of the cell (2 cm^2)
$D_{air\text{-}\alpha}$	binary diffusion coefficient ($cm^2\ s^{-1}$)
D_w	Fickian back-diffusion coefficient ($cm^2\ s^{-1}$)
F	Faraday constant (96,484 C mol^{-1})
g	gravity constant (9.81 m s^{-2})
I	current (A cm^{-2})
L	length of the packaging
M_m	molecular weight of the membrane (1100 g mol^{-1})
N_{BD}	back-diffusion molar flux (mol s^{-1})
N_d	electro-osmotic drag coefficient
N_{EO}	electro-osmotic drag molar flux (mol s^{-1})
P	pressure (atm)
P_{sat}	saturation pressure of water (atm)
P_w	partial pressure of water (atm)
RH	relative humidity
T_{cell}	temperature of the cell (°C)
W_α	mass fraction of specie α
$\delta_{membrane}$	width of the ionic membrane (cm)
ΔV_σ	drop of voltage due to ionic resistance of the membrane (V)
λ	water content of the membrane (mol H_2O/mol SO_3^-)
ν	kinematic viscosity of air ($m^2\ s^{-1}$)
ρ_m	density of the membrane (2.0 g cm^{-3})
σ	ionic conductivity of Nafion 117 ($\Omega^{-1}\ cm^{-1}$)
σ_{30}	ionic conductivity of Nafion 117 at 30 °C ($\Omega^{-1}\ cm^{-1}$)
$\bar{\sigma}$	mean ionic conductivity of the membrane ($\Omega^{-1}\ cm^{-1}$)
$\overline{Sh}_L^\alpha$	Sherwood number for specie α
$\bar{h}_m^\alpha$	mass transfer coefficient for specie α (cm s^{-1})
Ra_L^α	Raleigh number

Subscripts

∞	ambient conditions
s	surface of the cathode
α	species: H_2O, O_2, N_2
β	species: H_2O, O_2, N_2

2. Theory and modelling

A simple model of an air-breathing mPEMFC is realized to understand the water management phenomena involved. Because the main goal of the model is not to predict precisely the voltage drop in the cell but to highlight the general trends of water transport inside the Nafion® membrane, some assumptions are made to simplify the model.

First, the model represents the steady-state conditions and is one dimensional, since the water transport phenomena occurs mainly across and perpendicular to the membrane (x axis in Fig. 1). Secondly, a small amount of the water produced by the cell is generally evaporated by the anode flow [7,8], but this quantity is neglected to represent the dead-ended condition. Therefore, water is only evaporated at the cathode surface by natural convection. Thirdly, because of its size, temperature of a mPEMFC tends to be uniform and can be easily controlled by its packaging (material, area, etc.) [9], so it is considered to be isothermal. Finally, since mass transport resistance due to natural convection will dominate over diffusion, the porous electrodes and GDLs are considered as thin layers. Fig. 1 shows the different phenomena that the model takes into account. These include water production and consumption at the electrodes, water transport through the membrane, and evaporation from the cathode. This model assumes that no liquid water accumulates at the cathode or in the membrane, since flooding conditions must be avoided for proper fuel cell operation. The following sections will describe the influence of water content in the membrane on its ionic conductivity and water transport properties, then compute the water balance in the Nafion® to evaluate the water content and ionic resistance profiles through the membrane. Model predictions will then be presented as a function of current density and cell temperature.

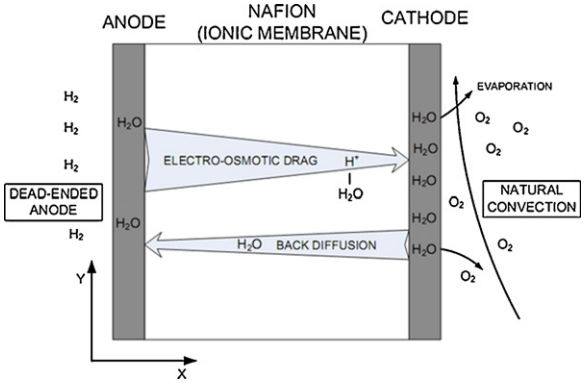

Fig. 1. Water transport phenomena and outside conditions taken into account in the 1D mPEMFC model.

2.1. Water content and ionic conductivity of Nafion®

The number of water molecules per charged sulfonic site in the Nafion® membrane, referred to as the water content (λ), is very important since it affects the ionic conductivity and the water transport properties in the membrane. The value of λ can vary from 2, when the membrane is dry, to 14 when it is saturated with water vapor. Water content is not uniform between the electrodes because its value depends on the local partial pressure of water, $P_w(x)$, and saturation pressure, P_{sat}, in the cell [10]. It is expressed by Eq. (1), for standard atmospheric conditions:

$$\lambda(x) = 0.043 + 17.81\frac{P_w(x)}{P_{sat}} - 39.81\left(\frac{P_w(x)}{P_{sat}}\right)^2 + 36.0\left(\frac{P_w(x)}{P_{sat}}\right)^3. \quad (1)$$

Water content of the membrane influences its ionic conductivity (σ), which is calculated as a function of $\lambda(x)$ and cell temperature, T_{cell} [10]:

$$\sigma(x) = \exp\left[1268\left(\frac{1}{303} - \frac{1}{273 + T_{cell}}\right)\sigma_{30}(x)\right] \quad (2)$$

where

$$\sigma_{30}(x) = 0.005139\lambda(x) - 0.00326. \quad (3)$$

The local ionic conductivity must be integrated over the total thickness of the membrane ($\delta_{membrane}$) to obtain the average ionic conductivity, $\bar{\sigma}$ (Eq. (4)). This value is then used to estimate the voltage drop caused by the membrane resistance ΔV_σ (Eq. (5)):

$$\bar{\sigma} = \frac{1}{\delta_{membrane}}\int_0^{\delta_{membrane}} \sigma(x)dx \quad (4)$$

$$\Delta V_\sigma = \frac{\delta_{membrane}}{\bar{\sigma}} I \quad (5)$$

The active area of the cell is represented by A and I is the current density (A m^{-2}).

Water content not only affects the total conductivity of the membrane, but also water transport phenomena inside the cell.

The equations used to estimate water content in the membrane as a function of current and temperature are presented in the next section.

2.2. Water transport in Nafion®

Three water transport phenomena can occur in the ionic membrane: permeation, electro-osmotic drag and diffusion. Permeation is the water flow caused by the differential pressure between the anode and the cathode. These pressures are assumed to be the same, so permeation is neglected.

The electro-osmotic drag, which represents the transport of water molecules carried by protons crossing the membrane, is proportional to the current density, I. Total water flux towards the cathode caused by electro-osmotic drag, N_{EO}, is computed with Eq. (6) where F is the Faraday number:

$$N_{EO} = N_d \frac{AI}{F}. \tag{6}$$

The value of the electro-osmotic drag coefficient N_d, which represent the number of water molecules carried per crossing proton, varies significantly in the literature. Some authors consider that N_d is a function of water content [10] and others evaluate it as a constant. Brüchi [11] showed that using a constant N_d allows computing of a realistic water profile inside the membrane. For this reason, in this paper, the value of unity suggested by Zawodzinski et al. [12] is used:

$$N_d = 1. \tag{7}$$

Since each proton that crosses the membrane carries one water molecule, two molecules are brought to the cathode by electro-osmotic drag for each water molecule that is produced by the electro-chemical reaction. This creates a water gradient inside the membrane that must be counterbalanced by the back diffusion flux, N_{BD}, to achieve a steady-state regime ($N_{EO} = N_{BD}$). The diffusion flux can be written as [13]:

$$N_{BD} = D_w(x) \frac{\rho_m}{M_m} \frac{dy}{dx} \tag{8}$$

where the diffusion coefficient of water in the membrane is expressed as:

$$D_w(x) = 0.0031\lambda(x)[\exp(0.28\lambda(x)) - 1]\exp\left(-\frac{2436}{T_{cell}}\right) \quad (\text{for } 0 < \lambda \leq 3) \tag{9}$$

$$D_w(x) = 0.000417\lambda(x)[1 + 161\exp(-\lambda(x))]\exp\left(-\frac{2436}{T_{cell}}\right) \quad (\text{for } 3 < \lambda \leq 17) \tag{10}$$

with, ρ_m as the density of the membrane and M_m its molecular weight.

The equilibrium between electro-osmotic drag and back-diffusion flux determines the total water content inside the membrane and therefore its conductivity. This balance is greatly influenced by the cell temperature because the water transport phenomena are not similarly affected by this factor.

2.3. Impact of temperature on water transport and ionic conductivity of the membrane

In most cases, the working temperature of mPEMFCs is considerably lower than for standard PEMFCs. The temperature difference between the cell and the ambient (ΔT) is obtained by combining the equations for generated thermal power by the cell (Q_g) with the heat dissipated by natural convection (Q_c):

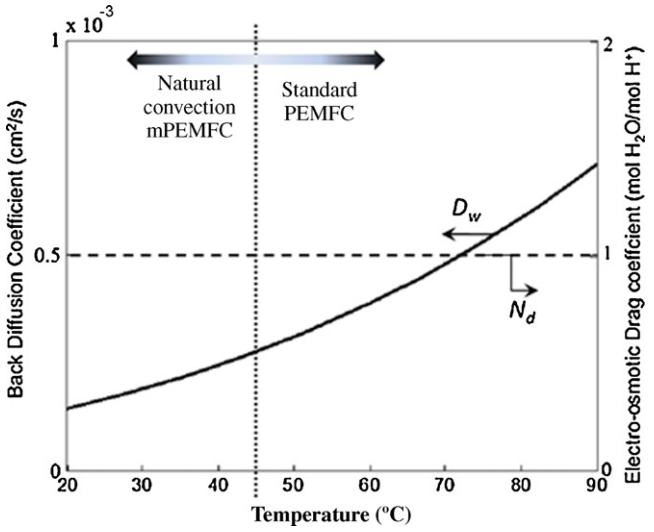

Fig. 2. Back diffusion and electro-osmotic drag coefficients as a function of temperature for a fully humidified membrane ($\lambda = 14$).

$$Q_g = P_w A_c \tag{11}$$

$$Q_c = \bar{h}_T A_p \Delta T \tag{12}$$

$$\Delta T = \frac{P_w}{\bar{h}_T} \frac{A_c}{A_p} \tag{13}$$

In smaller cells, the ratio of cell active area (A_c) to the external surface of the packaged device (A_p) tends to be lower, leading to little temperature difference between the cell and the environment. The heat transfer coefficient, $\bar{h}_T$, in a free convection situation, is proportional to $L^{1/4}$ (Section 2.4) where L is the characteristic length of the cell. Consequently, $\bar{h}_T$ increases when the dimensions of the cell reduce. Also, since air-breathing mPEMFCs are low power cells, P_w is small as well. All this leads to low working temperatures (20–40 °C for mPEMFCs compared to 50–90 °C for standard PEMFC) that have an important impact on water transport in the cell.

Unlike electro-osmotic drag, back-diffusion depends on temperature (Eqs. (9) and (10)). For similar water content, if the temperature decreases, the electro-osmotic drag flux remains unchanged while the back-diffusion flow drops (Fig. 2). At low temperature, electro-osmotic drag becomes dominant and the difference in water content between the anode and the cathode increases. Moreover, the ionic conductivity of the membrane also decreases with temperature (Fig. 3), boosting the impact of a high water content gradient between the electrodes. Under these conditions, anode drying can have a significant impact on the performances of the cell even with a saturated cathode because of the low back-diffusion flow. To quantify the impact of low temperature on the water content of the membrane, water transport relations in the membrane must be coupled to convection and diffusion equations at the cathode.

2.4. Water transport model formulation with natural convection

To define the water content throughout the membrane in a working cell, Eqs. (1)–(10) are linked to gas species (O_2, H_2O, N_2) mass transfer relations at the cathode. For diffusion of oxygen and water in ambient air at 25 °C, the Lewis number is near unity [9]. This means that the analogy between heat and mass transfer can be used and air species average mass transfer coefficient ($\bar{h}_m^{\alpha}$) can

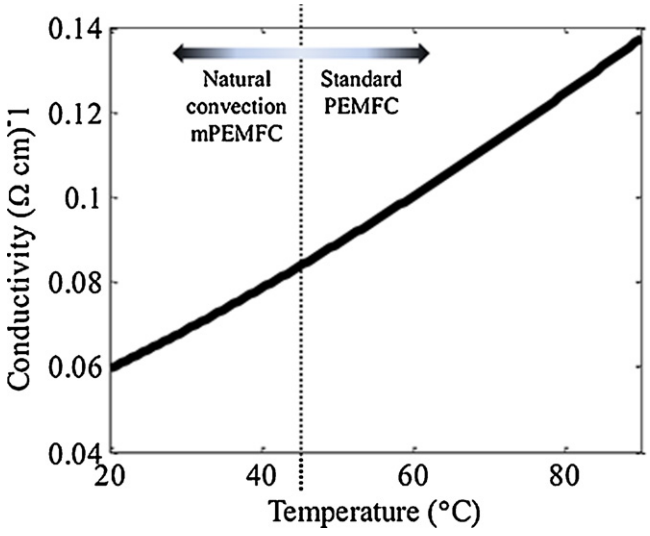

Fig. 3. Variation of the conductivity of a Nafion 117 membrane at $\lambda = 14$.

be determined with empirical relations. If the Sherwood number ($\overline{Sh}_L^{\alpha}$) is known, $\bar{h}_m^{\alpha}$ can be determined for each species (Eq. (14)).

$$\overline{Sh}_L^{\alpha} = \frac{\bar{h}_m^{\alpha} \cdot L}{D_{air\text{-}\alpha}} \tag{14}$$

Note that the Sherwood number is averaged over the surface of the cathode. Since the cell is small (1 cm × 2 × cm), large concentration gradients are not achieved in the in-plane direction. For example, water tends to distribute uniformly within the GDL at the cathode surface. This has been observed experimentally has water droplets are appearing at random sites when flooding occurs. Therefore, all non-dimensional numbers that are computed as well as mass transfer coefficients are averaged over the cathode surface. To determine the value of the Sherwood number for all species, the Rayleigh number (Ra_L^{α}) must be computed. Li et al. [14] have proposed relations to evaluate these numbers for mass transfer occurring on a vertical plate (Eqs. (15)–(17)):

$$\overline{Sh}_L^{\alpha} = 0.54 Ra_L^{\alpha 1/4} \tag{15}$$

$$\overline{Ra}_L^{\alpha} = \frac{g\gamma_{\alpha}(w_{\alpha\text{-}s} - w_{\alpha\text{-}\infty})L^3}{\nu D_{air\text{-}\alpha}} \tag{16}$$

$$\gamma_{\alpha} = \frac{M_{air} - M_{\alpha}}{w_{\alpha} M_{air} + ((1 - w_{\alpha})M_{\alpha})} \tag{17}$$

where g = gravitational acceleration; w = mass fraction of the specie; ν = air viscosity.

By combining Eqs. (14)–(17), a mass transfer coefficient can be calculated for each gas species:

$$\bar{h}_m^{\alpha} = \frac{0.54 Ra_L^{\alpha 1/4} \cdot D_{air\text{-}\alpha}}{L}. \tag{18}$$

Binary diffusion coefficients ($D_{air\text{-}\alpha}$) are computed with the relations of Bird [15]:

$$D_{\alpha\beta} = 10^{-4} \frac{a}{P} \left(\frac{T}{\sqrt{T_{c\alpha} \cdot T_{c\beta}}} \right)^{b} (P_{c\alpha} \cdot P_{c\beta})^{1/3} (T_{c\alpha} \cdot T_{c\beta})^{5/12} \times \sqrt{\frac{1}{M_{\alpha}} + \frac{1}{M_{\beta}}} \tag{19}$$

where a = empirical coefficient: 2.745×10^{-4} for polar gases and 3.640×10^{-4} for H_2O with a non-polar gas; b = empirical coefficient: 1.823 for polar gases and 2.334 pour H_2O for H_2O with a non-polar gas; P: outside pressure [atm]; T: gases temperatures [K]; T_c: critical temperature [K]; P_c: critical pressure [atm].

Table 1
Model input values.

Model parameter values	
M_m	1100 g mol^{-1}
ρ_m	2.0 g cm^{-3}
L	3 cm
P_{∞}	1 atm
RH_{∞}	0.5
A	2 cm^2
T_{∞}	22 °C
T_{cell}	25 °C
$\delta_{membrane}$	170 μm
ν	15.11×10^{-6} m^2 s^{-1}

With the values of the different $\bar{h}_m^{\alpha}$, Maxwell–Stefan relation is used to describe multi-species mass transfer by natural convection at the surface of the cathode:

$$\sum_{\beta=O_2,H_2O,N_2} (x_{\beta} \cdot N_{\alpha} - x_{\alpha} \cdot N_{\beta}) = -\Delta x_{\alpha} \cdot \frac{P}{RT_{cell}} \cdot \bar{h}_m^{\alpha} \tag{20}$$

where x, N and c are respectively the partial pressure, molar flux and concentration.

The model is split in two distinct sections, the convection at cathode surface and the diffusion through the membrane thickness. The key variable that links these sections is the molar fraction of water at the cathode x_{H_2O-c}, assumed to be constant through the thin electrode. The mass transport due to natural convection at the cathode surface is represented by Eqs. (14)–(20). An iterative process is used to calculate $\bar{h}_m^{\alpha}$ which allows us to compute the value of x_{H_2O-c} depending on external and operating conditions. To relate conditions at the cathode with water transport inside the membrane, total molar flux for oxygen consumption and water produced by the cell must be known. They are expressed by:

$$N_{O_2} = -\frac{IA}{4F} \tag{21}$$

$$N_{H_2O} = -\frac{IA}{2F} \tag{22}$$

Since it is considered that no water is leaving by the anode, electro-osmotic drag and back-diffusion flux must be equal to satisfy the permanent regime condition in the membrane. With x_{H_2O-c} known, the water content of the membrane at the cathode λ_c can be evaluated with Eq. (1). With this value and permanent regime conditions, water content profile $\lambda(x)$ is defined by integrating $d\lambda/dx$ with Eqs. (6)–(10).

To investigate the hypothesis that drying at the anode may be problematic in mPEMFC, the model is applied to a representative configuration. The mPEMFC has an active area of 2 cm^2 with a Nafion® 117 membrane. Table 1 shows the input values to the model.

Also, dry hydrogen feeds the anode by a dead-ended flow and oxygen is brought to the cathode by natural convection. This model can be used to investigate the water distribution across the membrane, and the potential for anode drying even when liquid water accumulates at the cathode.

2.5. Results of the analytical model

The simple 1D model, with the presented configuration, provides useful information on the water profile inside the membrane depending on ambient conditions, current and temperature of the cell. In this section, the effects of changing current will be discussed.

Fig. 4 presents the evolution of the water content profile across the membrane and the membrane resistance as a function of current density, for the configuration showed in Table 1.

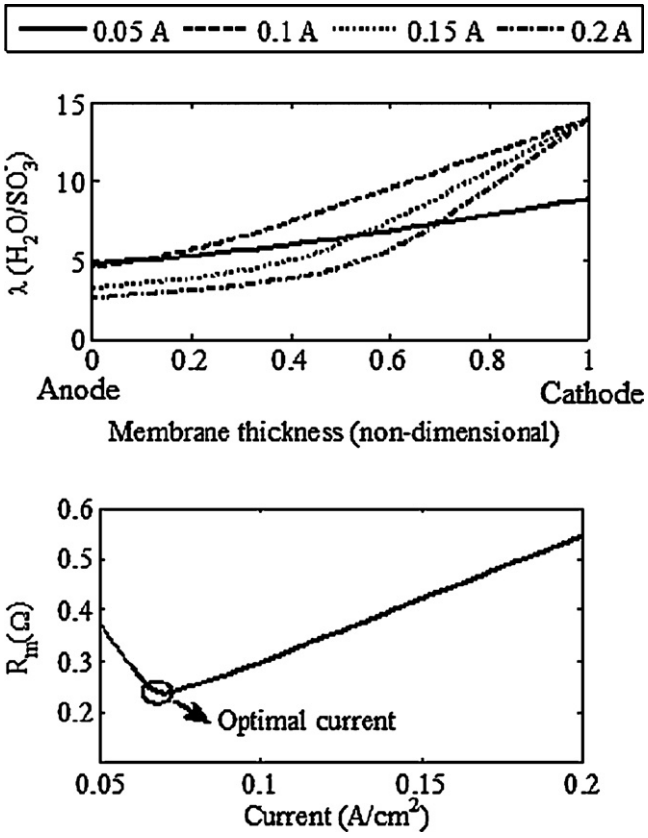

Fig. 4. Effect of current density on the water content profile (a) and ionic resistance (b) in a Nafion 117 membrane for T_{cell} = 25 °C.

At very low current (>0.05 A cm^{-2}), the membrane resistance ($R_m = \delta_{membrane}/\sigma A$) is relatively high because the cell does not produce enough water to humidify itself completely. This does not have a significant effect on the cell performance since the current is low and consequently, the voltage drop ΔV caused by the resistance of the membrane will not be significant. As the current increases, the rate of water formed at the cathode is sufficient to wet the membrane and the resistance drops. The resistance reaches a minimum (noted in Fig. 4) at which the cathode side of the membrane is fully humidified. Beyond this point, all the liquid water produced in excess at the cathode is expected to be wicked by the GDL to respect the permanent regime condition. Consequently, the cathode stays fully saturated (λ = 14) but the increase of the electro-osmotic drag (proportional to current) tends to dry the anode side of the membrane. This is better explained by writing the water balance in the membrane at steady state, $N_{EO} = N_{BD,}$ using Eqs. (6) and (8):

$$N_d \frac{AI}{F} = D_w(x) \frac{\rho_m}{M_m} \frac{d\lambda}{dx} \tag{23}$$

When the current increases, a larger gradient of water content is required to maintain sufficient back diffusion. Since the cathode side is saturated, this leads to a reduction of water content on the anode side. This assumes that the GDL is effective at removing liquid water from the electrode and allowing oxygen to diffuse when the current is increased.

It is interesting to explicitly compare the water content at the cathode, $\lambda_{cathode}$, to the one at the anode, λ_{anode}, if T_{cell} stays constant but I varies (Fig. 5). Three distinct phases appear in Fig. 5 depending of the current. The first section, defined as the wetting zone, is where both electrodes are slowly humidifying when current is increased because the cell can evaporates more water than it produce. As the current increases, the cell enters in its transition

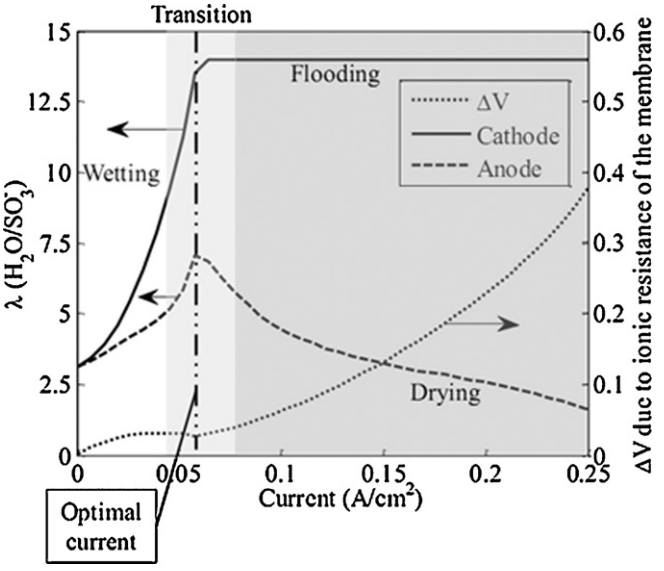

Fig. 5. Water content at the electrodes as a function of current density for T_{cell} = 25 °C. External temperature = 22 °C, RH = 50%.

zone where the electrodes get to their optimal working point. After this point, water must be removed from the cathode to prevent the oxygen pathways from being blocked. This can be done by allowing liquid water to drip or by using capillary structures to enhance the evaporation [3]. On the other side of the cell, the water content at the anode decreases as the electro-osmotic drag flux rises. Because the total water content of the membrane falls rapidly and that the current increases, the voltage drop due the ionic resistance of the membrane becomes significant and greatly affects the performances of the cell. The model suggest that for a mPEMFC working at low temperature the limiting current of the cell can be due to anode dry-out, if water is properly managed on the cathode [3].

Based on these results, it can be deduced that humidifying the anode will have a positive effect on the performance of the cell, potentially even when the cathode is flooding. Of course, water must be removed from the cathode's GDL to allow oxygen diffusion in steady-state operation. Conceptually, these requirements could be satisfied simultaneously by forcing water from the cathode to the anode. By preventing the cathode from flooding and the anode from drying, high and stable performances of mPEMFCs near ambient temperature should be achievable.

3. Experimental setup and test conditions

To validate the fact that cell performances increase by humidifying the anode, even if the cathode is flooding, an experimental characterisation was done with direct injection of water at the anode.

The 1 cm × 2 cm cell consists of a Nafion NR212 membrane (50 μm thick) with 0.3 mg cm^{-2} Pt loaded electrodes and 400 μm thick carbon cloth GDLs. The Membrane Electrode Assembly (MEA) is sandwiched in the same packaging used by Paquin and Frechette [9] and illustrated in Fig. 6. To ensure constant temperature of the cell, aluminum fins are added to the packaging to increase heat exchange with the ambient. In the back of the plexiglass support plate (part i of Fig. 6), a hole is drilled to insert the needle of a syringe. Liquid water is injected directly through this needle in the serpentine flow channel (1 mm of wide by 1 mm deep) on the anode side of the PEMFC by an automated syringe pump (Harvard Apparatus PHD 2000, Fig. 7). Dry hydrogen is fed to the anode with a test station built by *Fuel cell Technologies* at a stoichiometric ratio of 1.5 and oxygen is supplied to the cathode by natural convection of

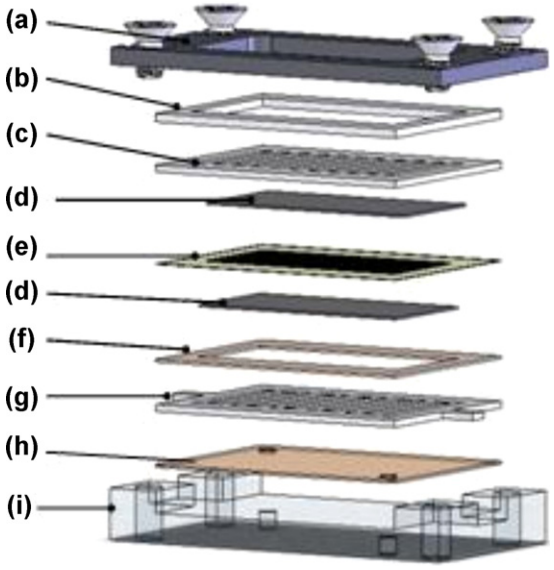

Fig. 6. Exploded view of the miniature PEMFC prototype. (a) Stainless steel support plate for cathode, (b) Grafoil® sheet, (c) Stainless steel grid for cathode, (d) GDL (SGL Carbon 10 BB), (e) MEA: catalyst coated NAFION® NRE 212 and loading of 0.3 mg Pt cm^{-2} from Ion Power, Inc., (f) seal to prevent lateral diffusion of hydrogen in anode GDL, (g) Stainless steel anode channel, (h) seal for anode flow, (i) plexiglass support plate for anode.

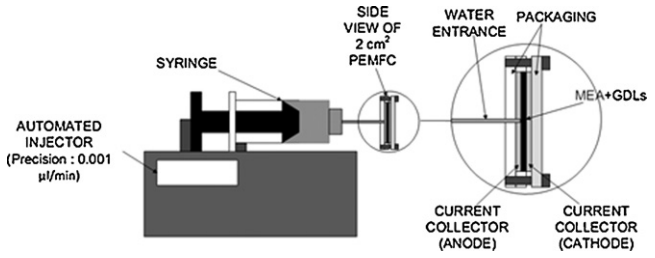

Fig. 7. Experimental setup for injection of liquid water directly at the anode of the mPEMFC while it is running.

ambient air. Uncertainty on the current and voltage measurement are ±0.003 A and ±0.003 V respectively.

Two different experiments were carried out with the conditions presented in Table 2. First, to show that anode is drying when the cathode is flooding, water is injected at the anode at various ratios and at constant current. Water is injected constantly with proportions of 2.5:1 to 5:1 (2.5–5 times the quantity of water that is produced at the cathode by the electro-chemical reaction) during 15 min and then stopped. The selected water injection ratios are similar in magnitude to what is removed from the anode by the electro-osmotic drag (Section 2.2). Voltage of the cell was plotted during 1 h to witness the effect of water injection and determine when the effect of the water injection fades away. The current density was fixed at $I = 0.175$ A cm^{-2} and temperature of the cell at 25 °C because at these conditions, water droplets are visible on the cathode showing signs of flooding.

Secondly, to compare the performances of the cell with and without water injection, *VI* curves were done by fixing the cell current for 30 min at each point of the polarization curve. The two test series were done with the same external conditions to ensure reproducibility of the results. For the polarization curve with water injection, a ratio of 5:1 is infused at the surface of the anode while it is running. This injection ratio is slightly higher than what is it removed from the anode by electro-osmotic drag (Section 2.2) and ensures a complete humidification of the anode.

Table 2
External and working conditions of the cell for the experiments.

Experimental conditions	
T_∞	22 °C
RH_∞	50%
T_{cell}	25 °C
H_2 flow	Dry, 1.5 (stoichiometric)

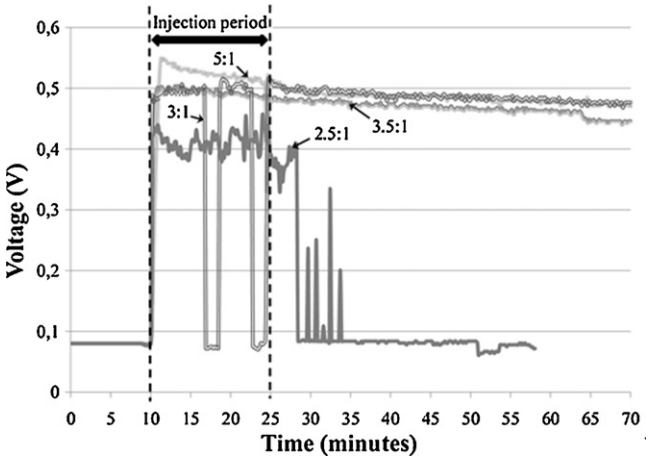

Fig. 8. Time response of the 2 cm^2 PEMFC during and after water injection at the specified ratios. Dry H_2, $st = 1.5$ (minimum flow = 4 sccm), Temp = 22 °C, RH = 50%, $I = 0.175$ A cm^{-2}.

4. Results and discussion

4.1. Water injection at the anode while the cathode is flooding

To see if electro-osmotic drag is responsible not only of flooding at the cathode but also drying of the membrane simultaneously, water is injected directly at the surface of the anode at a constant current. The results of this experiment showed in Fig. 8 prove that feeding the anode with liquid water when the cathode is flooding has high beneficial effect on the performances of the cell. Even at low injection rate (2.5:1), the voltage of the cell step up from 0.08 V to 0.4 V during the injection time. This is due to lower ionic resistance of the membrane cause by a better humidification. Still the membrane is not fully saturated because the positive effect of humidification disappears almost immediately when the injection is stopped and the voltage rises even more when the injection ratio is increased. At superior injection rates, the voltage increases up to 0.5 V and the effect of a 15 min injection stays for a longer period of time. This means that there is enough water injected to humidify the anode GDL and the membrane. At large ratios, however, the anode will eventually flood if water continues to be fed to it. Given this compromise, the optimal water injection ratio appears to be between 2.5:1 and 3:1 which corresponds approximately to the rate of water that is removed from the anode by the electro-osmotic drag (Section 2.2). This suggests that there is sufficient water available to humidify the anode if all the water at the cathode is redirected by an alternative pathway towards the anode.

4.2. VI curves

By comparing *VI* and power curves for the cell with and without water injection at the anode, it is possible to show the impact of humidifying the anode when the cathode is flooding (Fig. 9). The three zones introduced in Fig. 5 are also highlighted in Fig. 9. In the anode wetting and transition zones, water injection does not have a significant effect because the voltage drop due to resistance of the membrane is low (Fig. 5). When the current rises, the

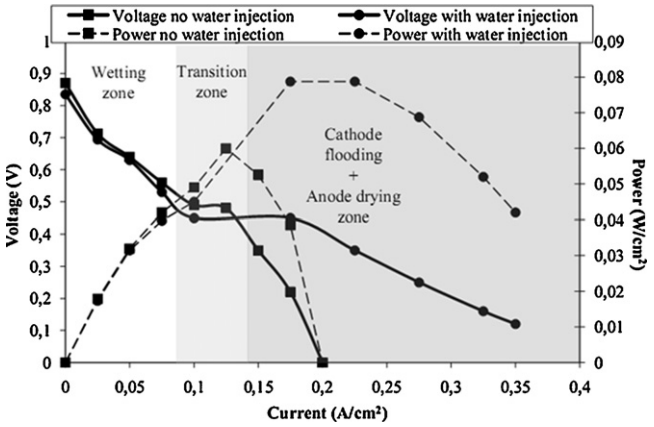

Fig. 9. *VI* and power curves for the 2 cm^2 mPEMFC with water injection (circles) and without (squares). Dry H_2, *st* = 1.5 (minimum flow = 4 sccm), Temp = 22 °C, RH = 50%.

voltage of the cell without water injection falls rapidly. This quick drop is generally associated with flooding of the cathode. In fact, in this third zone, water droplets are effectively forming at the surface of the GDL. However, it is in this part of the curve that the benefits of humidifying the anode are most apparent. By injecting liquid water at the anode, the ultimate current of the cell goes from 0.2 A cm^{-2} to 0.4 A cm^{-2} when the maximal power output rises from 0.06 W cm^{-2} to 0.08 W cm^{-2} even if the cathode continues to flood. This shows that water should be removed from the cathode to ensure stable voltage of the cell, and at the same time the membrane should be hydrated to reduce its ionic resistance and thereby increase the voltage of the cell.

5. Conclusion

In this work, it has been shown that a simple 1D model can highlight the general trends of water transport inside an air-breathing mPEMFC. With this model, it has been pointed out that the low working temperatures of mPEMFCs causes water management problems inside the cell. Temperature of the cell near ambient conditions not only generates flooding at the cathode by decreasing the evaporation rate but also simultaneously leads to drying of the membrane on the anode side by reducing the back-diffusion flow. Experimentally, humidifying the anode side by injecting water drastically improved the cell performance, confirming the proposed behaviour. Moreover, the required water injection rate at the anode is of the same magnitude of that removed from the membrane by electro-osmotic drag. This means that to increase the ultimate current and power density, excess water at the cathode should not be thrown away but redirected towards the anode. Water removal from the cathode is required for steady-state operation while water at the surface of the anode humidifies the membrane, decreases the ionic resistance and improves significantly the performances of the mPEMFC. It has been shown that by injecting water directly on the anode, the limiting current can double and power can be increased by 30%. The next step is to produce a device that would redirect the excess water from the cathode to the anode. In this way, no external water injection would be required.

Acknowledgements

This work was funded by the Natural Science and Engineering Research Council (NSERC) of Canada and the Canada Research Chair program.

References

[1] J.P. Meyers, H.L. Maynard, J. Power Sources 109 (2002) 76–88.
[2] Modroukas, D., Ph.D. thesis, Dept of Mech. Engg, Columbia University, 2006.
[3] D. Modroukas, V. Modi, L.G. Fréchette, J. Micromech. Microeng. 15 (2005) 193–201.
[4] T. Fabian, R. O'Hayre, S. Litster, F.B. Prinz, J.G. Santiago, J. Power Sources 195 (11) (2010) 3640–3644.
[5] U.H. Jung, S.U. Jeong, T.P. Ki, M.L. Hyang, K. Chun, W.C. Dong, H.K. Sung, Int. J. Hydrogen Energy 32 (17) (2007) 4459–4465.
[6] D. Chu, R. Jiang, J. Power Sources 83 (1–2) (1999) 128–133.
[7] N. Karst, V. Faucheux, A. Martinent, P. Bouillon, J. Laurent, F. Druart, J. Simonato, J. Power Sources 195 (4) (2010) 1156–1162.
[8] A. Schmitz, M. Tranitz, S. Eccarius, A. Weil, C. Hebling, J. Power Sources 154 (2) (2006) 437–447.
[9] M. Paquin, L.G. Frechette, J. Power Sources 180 (1) (2008) 440–451.
[10] T.E Springer, T.A. Zawodzinski, S. Gottesfeld, J. Electrochem. Soc. 138 (8) (1991) 2334–2342.
[11] F.N. Buchi, G.G. Scherer, J. Electrochem. Soc. 148 (3) (2001) 183–188.
[12] T.A. Zawodzinski, J. Davey, J. Valerio, S. Gottesfeld, Electrochim. Acta 40 (3) (1995) 297–302.
[13] J. St-Pierre, J. Electrochem. Soc. 154 (1) (2007) 88–95.
[14] P.-W. Li, T. Zhang, Q.-M. Wang, L. Schaefer, M.K. Chyu, J. Power Sources 114 (1) (2003) 63–69.
[15] R.B. Bird, W.E. Stewart, E.N. Lightfoot, Transport Phenomena, 2nd ed., Wiley, New York, 2002, p. 895.